Published in final edited form as:
Annu Rev Biochem. 2011 ; 80: 333–355. doi:10.1146/annurev-biochem-061009-091643.

BIOCHEMISTRY OF MOBILE ZINC AND NITRIC OXIDE REVEALED BY FLUORESCENT SENSORS

Michael D. Pluth, **Elisa Tomat**, and **Stephen J. Lippard**
Department of Chemistry, Massachusetts Institute of Technology, Cambridge, Massachusetts 02139

Stephen J. Lippard: lippard@mit.edu

Abstract

Biologically mobile zinc and nitric oxide (NO) are two prominent examples of inorganic compounds involved in numerous signaling pathways in living systems. In the past decade, a synergy of regulation, signaling, and translocation of these two species has emerged in several areas of human physiology, providing additional incentive for developing adequate detection systems for Zn(II) ions and NO in biological specimens. Fluorescent probes for both of these bioinorganic analytes provide excellent tools for their detection, with high spatial and temporal resolution. We review the most widely used fluorescent sensors for biological zinc and nitric oxide, together with promising new developments and unmet needs of contemporary Zn(II) and NO biological imaging. The interplay between zinc and nitric oxide in the nervous, cardiovascular, and immune systems is highlighted to illustrate the contributions of selective fluorescent probes to the study of these two important bioinorganic analytes.

Keywords

cell imaging; fluorescent probes

1. INTRODUCTION

The interface between inorganic chemistry and biology is an exciting one. All living systems employ inorganic ions and molecules for biological function. Metal cations, inorganic anions, and small-molecule gases interact with biological macromolecules to drive a multitude of structural and catalytic processes. Of much current interest are the dynamic signaling roles of a variety of inorganic species, which drive physiological processes or, when uncontrolled, trigger pathology. The present review focuses on mobile forms of the divalent zinc cation and the gaseous nitric oxide radical as two prominent examples of inorganic species that participate in biological signaling networks in a manner that is not fully elucidated. The study of such signaling pathways can benefit greatly from novel techniques that detect the time- and position-sensitive locale of biological analytes in live cells and tissues. Small-molecule fluorescent probes, in particular, can respond in a direct and selective manner to specific analytes. As such, they provide a valuable means to study the generation, accumulation, and translocation of metal ions and other inorganic agents in biology with both spatial and temporal resolution. As the fidelity of techniques to study

DISCLOSURE STATEMENT

The authors are not aware of any affiliations, memberships, funding, or financial holdings that might be perceived as affecting the presentation of this review.

important bioinorganic analytes increases, multifaceted signaling pathways have emerged in biological regulation. In this context, selective fluorescent probes for zinc and nitric oxide are revealing the dichotomous and often interconnected roles of these species in the nervous, cardiovascular, and immune systems.

The divalent zinc cation, Zn(II), is ubiquitous in biology. Current database-mining techniques estimate that approximately 10% of the human genome encodes for the zinc proteome (1). Lewis acidic, redox inert in the biological medium, and adaptable to different coordination geometries, this metal cation plays a structural and catalytic role in the biochemistry of numerous metalloproteins (2). Moreover, zinc maintains a highly dynamic role in cell biology owing to rapid ligand exchange reactions that characterize its coordination chemistry (3). The intracellular pool of mobile zinc, variously known as free, chelatable, or loosely bound zinc, is regulated by several proteins, including metallothioneins (MTs) and zinc transporters of the ZnT and Zip families (4, 5). This zinc pool is capable of regulating other proteins and cellular processes through fluctuations of its local concentration. The origins and consequences of such zinc signals are central to human physiology and pathology (6, 7).

In the central nervous system, some glutamatergic nerve terminals feature synaptic vesicles containing millimolar quantities of zinc. Release of this vesicular zinc pool triggers signaling pathways that impact physiological functions, including synaptic plasticity, transmission, and long-term potentiation, as well as neuronal death processes connected to ischemia, epilepsy, and Alzheimer's disease (8–11). In pancreatic β-cells responsible for controlling glucose levels in blood and central to the study of diabetes, zinc is involved in multiple aspects of insulin metabolism, exemplified by the concomitant release of insulin and zinc from secretory vesicles (12–14). In the prostate glandular epithelium, zinc accumulation is essential for normal citrate production, and changes in mobile zinc concentrations parallel the metabolic changes that lead to the development of prostate malignancy (15–18).

In similar fashion to zinc, the biosynthesis and potentiation of nitric oxide (NO) is highly regulated. Although recognized originally as an environmental pollutant arising from incomplete combustion of nitrogen-containing molecules, NO is now understood to play important and diverse roles in biology. After the initial discovery in 1987 that NO is the endothelium-derived relaxing factor in the cardiovascular system (19, 20), its multifaceted roles in physiology and disease have grown to include prevalent functions in the cardiovascular, immune, and nervous systems (21–27). Biosynthesized from L-arginine, NO is ubiquitous in bacteria, plants, invertebrates, and mammals. Nitric oxide synthase (NOS), a heme-containing enzyme, catalyzes the oxidation of L-arginine to L-citrulline with concomitant consumption of one equivalent of O_2 and subsequent release of NO. Two NOS isoforms, neuronal NOS (nNOS, type I) and endothelial NOS (eNOS, type II), are calcium dependent and expressed constitutively, whereas the third isoform, inducible NOS (iNOS, type III), is calcium independent and expressed in cells associated with immune response upon exposure to cytokines and/or endotoxins. The three NOS isoforms provide a large range of biological NO concentrations, from nanomolar, for nNOS and eNOS, to micromolar for iNOS. Although NOS was originally thought to be the sole source of biological NO, recent work indicates that nitrite (NO_2^-) reduction is another source of its biosynthesis (28, 29). After initial generation, NO diffuses rapidly from its point of origin, with an average lifetime from milliseconds to seconds, before reacting with, and often altering the function of, other biomolecules.

Much of the chemistry of biological NO is associated with its potentiation because misregulation leads to numerous pathologies. For example, hypertension, arteriolosclerosis,

and impotence have all been associated with an underproduction of NO, whereas diabetes, stroke, septic shock, multiple sclerosis, and cancer are connected with its overproduction (30–38). Furthermore, high levels of nitric oxide can lead to the proliferation of downstream reactive NO species (RNOSs), such as NO_2^- or peroxynitrite ($ONOO^-$). RNOSs have been implicated in carcinogenesis and several neurological disorders, including Alzheimer's, Parkinson's, and Huntington's diseases (39, 40). As the biological understanding of NO evolves, it is apparent that other NO-derived species, such as nitrosothiols, $ONOO^-$, nitrogen dioxide (NO_2), dinitrogen trioxide (N_2O_3), nitroxyl (HNO), NO_2^-, and nitrate (NO_3^-), may also have important biological functions (28, 41, 42).

In organ physiology, both zinc and NO dynamics are connected to multiple upstream and downstream pathways through interactions with proteins, small-molecule modulators, and other signaling agents. Recent information about the intersecting pathways of zinc and nitric oxide provides exciting clues to the functional schemes of these inorganic species in neurobiology, lung and heart physiology, and immunology. The complexity of such network maps motivates the development of increasingly sophisticated approaches to sensing and imaging these inorganic species in live cells and tissues. In the present review, we highlight the current knowledge of the interplay between zinc and nitric oxide as it has emerged from studies employing, among other tools, fluorescent detection systems to track these inorganic species in biological settings. The most widely used probes for both analytes are covered, and an emphasis is placed on promising new developments and unmet needs of contemporary imaging studies of mobile Zn^{2+} and NO.

2. SENSING STRATEGIES

Fluorescence imaging of biological analytes offers an attractive platform for monitoring biological processes in real time with high spatial resolution. Ideally, fluorescent probes should maintain sufficient water solubility, membrane permeability, and low toxicity for biocompatibility. Furthermore, low-energy excitation/emission and a large dynamic range between the on and off states of the probe greatly enhance the efficacy of such indicators. Depending on the nature of the experiment, sensor properties, such as reversibility, cell trappability and selectivity, can impact experimental conditions and results. The understanding of biological zinc and nitric oxide have benefited greatly from the development of fluorescent probes. Readers interested in the full landscape of fluorescent sensors available for mobile zinc (43–51) and nitric oxide (52–60) are referred to these recent reviews. Below, we present a gallery of fluorescent zinc and nitric oxide indicators used most widely for the study of the Zn/NO synergism and selected recent contributions that address current challenges in zinc or NO imaging and may provide useful tools for future studies.

2.1. Fluorescent Sensors for Mobile Zinc

Most zinc indicators employed in fluorescence microscopy experiments are intensity-based sensors that respond to zinc coordination with an increase, or rarely a decrease, in fluorescence emission intensity without a significant shift in emission wavelength. Although such fluorescence turn on or turn off is readily imaged by current microscopy instrumentation, zinc quantification is complicated by the dependency of intensity on dye loading, cell thickness, photobleaching, and sensor diffusion to the extracellular medium, and uneven cellular distribution of the indicator. Large changes in emission intensity upon analyte binding, which reflect the dynamic range of the sensor, are preferred because they provide better contrast in fluorescence micrographs. Low background and high turn-on emission define the dynamic range.

2.1.1. Turn-on fluorescent sensors for mobile zinc—Early fluorescent indicators employed in experiments to investigate biologically mobile zinc were based on 8-substituted quinoline platforms. For example, the formation of a fluorescent complex with 8-hydroxyquinoline allowed for the detection of zinc in human plasma and urine (61) and, by fluorescence microscopy, in the granules of cultured human leukocytes in the late 1960s (62). Since then, the quinoline derivative 6-methoxy-8-*p*-toluenesulfonamidequinoline (TSQ) (Figure 1) has been employed in many contexts for zinc bioimaging, including some of the earliest observations of zinc in brain tissue by fluorescence microscopy (63). Its analog Zinquin (Figure 1), available in both a carboxylic acid (Zinquin-A) and an ethyl ester form (Zinquin-E), retains a similar photophysical profile but with improved cell staining and retention properties (64). Zinc sensors of the 8-substituted quinoline family have detection limits in the picomolar range and large (up to 100-fold) fluorescence turn-on responses. The zinc-binding properties of such probes, however, are complicated by the tendency of these bidentate ligands to form a mixture of 1:1 and 2:1 complexes (65). Furthermore, quinoline-based indicators require excitation with UV light, which can result in both cellular photodamage and autofluorescence, thus limiting the applicability of such probes in live-cell experiments.

Fluorescein-based sensors constitute the largest family of indicators for biological zinc. The success of these probes has relied on the stability, water solubility, brightness, and visible-light excitation/emission of the fluorescein platform, as well as on the versatility of their modular design based on a fluorophore-spacer-receptor scheme. The receptor units are built around an electron-rich group, typically a secondary or tertiary amine, which quenches the fluorophore by photoinduced-electron transfer (PET) in the absence of the metal ion. The palette of available zinc sensors offers a selection of probes responsive in the desired concentration range and selective for zinc over other competing ions.

In the design of probes of the large Zinpyr (ZP) family (48), receptors based on the di(2-picolyl)amine (DPA) ligand were tethered to various fluorescein scaffolds. The first and most widely used member of this series, ZP1 (Figure 1), offers good cell permeability and optical brightness, zinc affinity in the low nanomolar range, and a fivefold increase of fluorescence quantum yield upon zinc binding (Φ_{free} 0.17, Φ_{Zn} 0.87) (66, 67). Because protonation of the basic receptor units can influence the PET quenching process, sensors of the ZP family are pH sensitive. Potentiometric and fluorometric experiments on ZP1 correlated its pH-dependent fluorescence response to a pK_a value of 7.0 for one of the protonation equilibriums of the system (67). This event results in a relatively high background fluorescence corresponding to partially protonated ZP1 at cellular pH. The background fluorescence can be attenuated, at least in some applications, by precomplexation of ZP1 with Mn(II). This paramagnetic ion quenches the fluorophore in the zinc-free state and is promptly replaced by Zn(II) ions both in vitro and in live cells. This displacement provides an improved turn-on response and better contrast in fluorescence microscopy experiments (68).

Sensors of the ZP and the related families of sulfur-containing ZS sensors (69) and quinoline-containing QZ sensors (70) span a wide range of zinc affinities and dynamic ranges (48). In addition, the pyrazine-containing ZPP1 (Figure 1) can provide an in vitro determination of zinc concentration in biological fluids through fluorometric titration experiments (71). For example, in experiments using zinc as a cancer biomarker in a transgenic mouse model of prostate adenocarcinoma, ZPP1 was used to quantitate zinc concentrations in prostate cell lysates and mouse prostate extracts (18).

Functionalization of the bottom ring of the fluorescein scaffold defines the ZnAF family of sensors carrying pyridine-rich receptors of varying denticity, chelate-ring size, and steric

bulk (72). Constructs of this series cover a large spectrum of zinc affinities (73); however, coordination of zinc does not fully restore the fluorescein emission, and the quantum efficiencies of zinc complexes of the ZnAF probes generally remain below 0.4 in neutral aqueous solution. One of the first members of this family, ZnAF-2 (Figure 1), exhibits nanomolar affinity for zinc and low pH-independent background fluorescence in the absence of zinc ions (72). ZnAF-2 is a membrane-impermeant indicator that can be employed to monitor extracellular zinc release.

Several zinc sensors are based on the scaffold of established biocompatible calcium indicators. In Newport Green DCF (Figure 1), for example, the calcium-binding BAPTA [1,2-bis(o-aminophenoxy)ethane-*N,N,N′,N′*-tetracetic acid] unit of Calcium Green™-1 is replaced with an aniline-fused **DPA** receptor (74). Newport Green DCF accommodates the softer and less oxophilic zinc cation with micromolar affinity and high selectivity over calcium and magnesium, although significant turn-on responses to nickel and cobalt have been recorded (75). A close relative of the BAPTA-based calcium sensor Fluo-4, FluoZin-3 (Figure 1), features only three of the four *N*-acetate groups of the original probe, a modification that produces greatly reduced affinity for calcium and nanomolar affinity for zinc (76). FluoZin-3 responds to zinc binding with a 200-fold increase in fluorescence emission and, in spite of its similarity to BAPTA-based receptors, is not perturbed by millimolar calcium concentrations (77). The rhodamine-based analog of FluoZin-3, RhodZin-3 (Figure 1), allows zinc detection at longer wavelengths with a 75-fold turn-on response (40). Although RhodZin-3 is membrane impermeant, the acetoxymethyl ester derivative is cell permeable and localizes in the mitochondria of eukaryotic cells, thus allowing study of mitochondrial zinc pools (40).

2.1.2. Ratiometric fluorescent sensors for mobile zinc—A major focus of current efforts in zinc sensor development is the design of ratiometric indicators (45, 49). Such probes respond to analyte binding with a shift of the corresponding excitation and/or emission profiles. Because each ratio of emission and/or excitation intensity at two chosen wavelengths corresponds to a specific analyte concentration, ratiometric sensors can be used to determine zinc concentrations in dual excitation or dual emission experiments. Systems of this type can supply valuable information on transient zinc levels in live cells or tissues, provided that the receptors have sufficiently rapid and reversible binding kinetics. Although several ratiometric, mostly UV-excitable probes for zinc in aqueous solution have been reported in the past decade (45, 46, 76), none has found wide applicability in zinc bioimaging.

In two recent examples of visible-wavelength-excitable sensors that have been tested in live-cell imaging experiments, coordination of zinc by the DPA unit is enhanced by additional interactions with heteroatoms of the fluorophore scaffold. In ZnIC (Figure 2), DPA-bound Zn(II) interacts with an iminocoumarin moiety, thereby influencing the internal charge transfer process connected to the fluorescence emission (78). In the amide-DPA sensor ZTRS (Figure 2), zinc coordination induces tautomerization of the amide moiety and causes a red shift of the emission profile of the naphthalimide fluorophore directly connected to the amide nitrogen atom (51).

Several promising ratiometric systems are based on zinc-induced modulation of intramolecular Förster resonance energy transfer (FRET). For example, the fluorescein-rhodamine construct **1** (Figure 2) relies on a zinc-induced ring opening of a rhodamine spirolactam, thus restoring emission of the rhodamine fluorophore and resulting in FRET between the xanthenone dyes. This modulation provides highly selective zinc detection over a large concentration range (from 2.0×10^{-7} M to 2.0×10^{-5} M) by measuring the ratio of the well-separated emission intensities of the two fluorophores (79).

A versatile FRET-based sensor design features a pair of autofluorescent proteins separated by a zinc-binding domain in which the conformational changes caused by zinc coordination affect the FRET efficiency of the system and result in a ratiometric signal (50). Such protein-based sensors can be genetically encoded by common molecular biology protocols and can be fused to localizing sequences that anchor the biosensor to a targeted cellular site. For instance, site-directed FRET-based biosensors were employed to detect zinc in the mitochondria of hippocampal neurons (80) and in the insulin-containing granules of pancreatic β-cells (81).

In an alternative approach to sensor localization, protein-labeling methodologies (82, 83) can be used to tether small-molecule indicators to protein tags genetically directed to a cellular compartment of choice. In this fashion, the *S*-nitroso-*N*-acetylpenicillamine (SNAP) tag (84) was employed to direct fluorescein-based sensor ZP1 to the Golgi apparatus and the mitochondria of live HeLa cells (85). If combined with ratiometric detection, sensor localization strategies will provide powerful tools for the dynamic description of zinc signals with nanoscaled subcellular resolution. The lower limit of resolution for imaging by light microscopy (~200 nm), which is increased by spatial averaging of the signal from freely diffusing indicators, allows visualization of organelle “microdomains” in eukaryotic cells, but it does not permit the study of smaller structures. Conversely, the genetic tethering of sensors to specific subcellular compartments can illuminate “nanodomains,” such as secretory granules and synaptic clefts, and allow one to distinguish between contiguous compartments within the same structure. Only zinc’s presence at such a nanodomain will trigger fluorescence.

2.2. Fluorescent Sensors for Nitric Oxide

The special physical properties of NO, such as its gaseous nature, limited water solubility (~1.7 mM), complex oxidation chemistry, diverse biological concentrations, and radical character, offer challenges in the design of selective probes for its detection. Classical techniques, such as electron paramagnetic resonance spectroscopy, for identifying free radicals lack the sensitivity and spatial resolution for use in live cells. Chemical traps for NO that form stable nitroxide radicals, such as fluorescent nitric oxide chelotropic traps based on the reaction of NO with *o*-quinodimethanes, have been developed but often suffer from problems with biological selectivity, sensitivity, and toxicity (86–88). Although NO-selective electrodes are valuable tools for tissue and whole blood measurements, they lack the spatial resolution and noninvasiveness required for many sensing applications. By contrast, optical methods for NO detection and quantification have produced increasingly accurate tools for elucidating the numerous roles of biological nitric oxide.

2.2.1. Organic probes for nitric oxide—The Griess assay, which relies on the reaction of NO_2^-, an oxidation product of NO, with sulfanilic acid and α-naphthalene under acidic conditions to produce an azo dye quantifiable by absorption spectroscopy, was one of the early methods for optical detection of NO (89, 90). This method allows for quantification of NO_2^- concentrations based on a calibration curve with a lower detection limit of approximately 0.5 μM. Refined variants of the Griess assay using sulfanilamide and *N*-(1-naphthyl)ethylenediamine produced a more sensitive and reproducible assay. Because the Griess assay is a bulk measurement and measures NO indirectly, determination of background NO_2^- cellular concentrations is important for reliable quantification.

By comparison to absorption-based measurements, fluorescent probes offer a class of important tools for cell culture, tissue slice, and whole-animal studies resulting from their sensitivity, optical resolution, generally available instrumentation, and ease of use. In the development of small-molecule fluorescent probes for nitric oxide, two distinct strategies

have emerged. The first, and more widely used, is based on entirely organic probes in which an oxidation product of NO, such as N_2O_3, reacts with a functional group to modulate the fluorescence (91). Such probes often result in bright (50–150-fold) emission enhancement in the presence of nitric oxide under aerobic conditions. A second strategy for devising fluorescence probes for nitric oxide is the use of transition metals to mediate reactivity of an emissive dye with NO. Such probes benefit from faster reaction times with NO owing to metal-mediated reactivity, but these probes can be less bright than purely organic probes when comparing their on and off states.

Numerous fluorescent probes for nitric oxide utilize the electron-rich 1,2-diaminobenzene moiety, which reacts with oxidization products of NO to form an electron-poor triazole (Figure 3). Introduction of a diamine unit to a fluorophore generally results in PET from the amine lone pairs to the excited fluorophore to quench the emission. Conversion of the diamine to an aryltriazole lowers the energy of the nitrogen lone pairs, thereby abolishing the PET pathway and restoring fluorophore emission. An early example of this reactivity for NO detection used 2,3-diaminonaphthalene (DAN) (Figure 3), which is converted to the fluorescent 2,3-naphthotriazole upon exposure to NO in an aerobic environment (92, 93). The cellular viability of DAN, however, is reduced by the required high-energy UV excitation and emission. This assay has been optimized as a biological NO_2^- assay, with a detection limit of approximately 10 nM, thereby providing increased sensitivity over the Griess assay (92).

The most common NO probes rely on the same aryldiamine-to-triazole conversion manifold but make use of biologically compatible fluorescein dyes. Diaminofluoresceins (DAFs) (Figure 3), incorporating the *o*-diamine moiety on the lower fluorescein ring, are selective for NO over NO_3^-, $ONOO^-$, H_2O_2, and O_2^- under aerobic conditions and maintain a 5-nM NO detection limit (94–96). Such probes benefit from visible excitation wavelengths, thus limiting interference from cellular autofluorescence and minimizing tissue damage during imaging. As in the Griess assay, DAF-based probes do not measure NO directly but rather monitor its oxidation products, such as N_2O_3. Their applicability is therefore limited in hypoxic cellular environments. Measurement of NO can be perturbed by the presence of dehydroascorbic acid or ascorbic acid, which form products with emission profiles similar to that of NO-derived triazoles, or by intracellular reductants, such as homocysteine and reduced glutathione (76, 97). Similarly, divalent cations increase the fluorescence of DAF probes prior to triazole formation, potentially complicating an observed emission (98). Although the parent DAF probes are cell membrane impermeable, esterification of the phenolate oxygen atoms imparts cell permeability (DAF-2 DA) (Figure 3). Upon cellular uptake, hydrolysis by intracellular esterases releases the active DAF-2 probe. The fluorescence of the triazole product, however, is pH dependent owing to protonation of the secondary amine of the triazole. This limitation can be attenuated by monomethylation of one of the diamine nitrogens and partial fluorination of the fluorescein platform (DAF-FM) (Figure 3) both to change the basicity of the triazole product and to increase its photostability (99). Much like the parent DAF probes, esterification of the phenolic oxygen atoms (DAF-FM DA) (Figure 3) results in a cell-permeable and trappable probe.

Other fluorophores have also been functionalized with diaminobenzene moieties to effect NO sensing. Diaminorhodamines (DARs) (Figure 3) (100) exhibit improved excitation profiles, photostability, and pH tolerance when compared to **DAF** analogs. Optimization of cell membrane permeability, intracellular hydrolysis rates, and intracellular localization led to the development of DAR-M, incorporating an acetoxymethyl ester to impart cell permeability and trappability, as well as nitrogen alkylation to lower the pH sensitivity of the triazole fluorescence.

Red fluorescent NO probes have also been developed based on the 1,2-diaminoanthraquinone (DAQ) (Figure 3) platform. DAQ itself is nonfluorescent, but conversion to the triazole ^{1}H-antra[1,2*d*]-[1,2,3]-triazole-6,11-dione (ATD) results in bright fluorescence (101, 102). DAQ effectively responds to both intra- and extracellular NO, and unlike the DAF triazole product, ATD is insoluble in water and precipitates upon formation, thus eliminating passive diffusion from the point of generation. This property allows for its fluorescence to be investigated even in fixed tissues. For other desired properties, such as pH insensitivity or longer-wavelength emission, researchers have utilized the *o*-diamine/NO reactivity manifold. Probes based on the BODIPY framework, such as DAMBO-P^{H} or DAMBOO (Figure 3), were developed that have higher NO sensitivity than DAF analogs, are pH insensitive over physiologically relevant acidities, and display a larger Stoke's shift (103, 104). Near-IR probes based on diaminocyanines (Figure 3) have also been developed to limit cellular damage and autofluorescence during imaging (105). Numerous other probes bearing the *o*-diaminobenzene motif, including modified calcium sensors (106), luminescent ruthenium complexes (107), and near-infrared emissive single-walled carbon nanotubes (108), are available. Similarly, the reaction of aerobic NO with a primary amine, followed by electrophilic aromatic substitution on the formed nitrosamine, has been used to generate a fluorescent conjugated diazo ring scaffold with excellent selectivity for NO over other reactive oxygen and nitrogen species (109).

2.2.2. Transition-metal-based probes for nitric oxide—An alternative approach to NO sensing utilizes transition-metal-mediated NO reactivity and has resulted in several probes based on Cu(II)-fluorophore scaffolds (Figure 4). In such systems, coordination of a paramagnetic Cu(II) ion by a sensor moiety carrying a secondary amine quenches emission of the fluorophore prior to reaction with NO. Upon reaction with NO, Cu(II) is reduced to Cu(I) with concomitant deprotonation and nitrosation of the secondary amine, which lowers the energy of a quenching lone pair on the nitrogen atom, thus diminishing PET quenching in the *N*-nitrosated product. Such probes select for NO over other reactive oxygen and nitrogen species, although some nonspecific but attenuated reactivity is often observed with other radicals such as H_2O_2 and NO_2. Unlike the *o*-diaminoarene sensing strategy, the Cu(II)-mediated reactivity does not require oxygen, which makes such probes potentially useful for imaging NO in hypoxic environments, such as those associated with carcinogenesis.

The CuFL1 platform (Figure 4) is based on a fluorescein dye with a pendant amino-quinoline moiety to bind Cu(II) (110–112). CuFL1 reacts directly and quickly with NO to result in a 16-fold emission turn on; the probe maintains selectivity for NO over other **RNOS** such as NO_2^-, NO_3^-, H_2O_2, HNO, $ONOO^-$, O_2^-, and ClO^-. Upon treatment with NO, Cu(II) is reduced to Cu(I) with concomitant nitrosation of the secondary amine leading to a fluorescence enhancement with first-order dependency on NO concentration (113). The CuFL probe has been used to image endogenously produced nitric oxide in Raw 264.7 macrophages, SK-N-SH neuroblastoma, the gram-positive *Bacillus subtilis*, and *Bacillus anthracis* (114, 115). Modification of the FL1 platform to generate a symmetric probe (FL2) (Figure 4) significantly increased the dynamic range (116). Introduction of ester groups on the two upper-ring quinolines resulted in a cell-trappable version of FL2 (FL2E) (Figure 4) that has been used to image endogenous NO in Raw 264.7 macrophages, SK-N-SH neuroblastoma, and olfactory bulb brain slices (117).

The use of Cu(II)-mediated *N*-nitrosation has also been applied to detect endogenous NO with the blue fluorophore MNIP (Figure 4) in Raw 264.7 macrophages and ASHI mouse liver slices (118). Numerous other small-molecule transition-metal complexes, including those of Co(II), Fe(II), Ru(II), and Rh(I), have been developed as nitric oxide sensors, although they have not been employed in live cells (112, 119–123). The strategy of binding

NO directly to a metal center also offers an attractive platform for devising reversible probes to detect nitric oxide, and NO release from such compounds has been amply documented (124–126).

2.2.3. Genetically encoded probes for nitric oxide—In addition to small-molecule transition-metal-based probes for NO, numerous constructs have been devised that use genetic encoding of NO-reactive proteins often containing transition-metal NO-reactive sites. An example is a fusion of two mutant green fluorescent proteins (GFPs) joined by an **MT** domain, which functions as an NO indicator. The FRET response between the mutated GFPs in response to the conformational change of MT upon reaction with NO provides a visible readout (127). Similarly, a selective NO sensor based on a GFP-labeled heme domain of soluble guanylyl cyclase (sGC) has been developed (128, 129). Upon NO binding to sGC, a linear and reversible response occurs owing to changes in the quantum yield of the GFP. In another strategy, fluorescent probes for guanosine 3′,5′-cyclic monophosphate (cGMP), and thus indirectly for NO, have been explored by attaching a cyan fluorescent protein and a yellow fluorescent protein at the N terminus and C terminus, respectively, of cGMP indicator proteins (130–133). FRET between the two GFPs increases with NO concentration as the result of amplification of the cGMP concentration. In addition to the high level of NO sensitivity, the binding of NO to sGC is reversible, reporting both increases and decreases in biological NO.

3. INTERPLAY OF ZINC AND NITRIC OXIDE IN BIOLOGY

3.1. Nervous System

The involvement of both Zn(II) and NO in a variety of neurological dysfunctions such as Alzheimer's disease, as well as the neurotoxic effects of both inorganic species, has sparked interest in studying the interplay between these two analytes in the central nervous system. Treatment of hippocampal neurons with exogenous NO donors, including sodium nitroprusside or the spermine-nitric oxide complex, resulted in mobilization and accumulation of Zn(II) in brain tissue, as detected by TSQ fluorescence and Timm staining (134). Zinc accumulation was observed in perikarya, axons, interneurons, and dentate granule cells two hours after injection with sodium nitroprusside or spermine-nitric oxide complex. Depending on the NO donor, differential staining of the pyramidal neurons, interneurons, or dentate gyrus was observed. Injection of the zinc chelator *N,N,N′,N′*-tetrakis(2-pyridylmethyl)ethylenediamine (TPEN) prior to NO-donor administration abolished zinc staining.

Treatment of neurons in primary cerebrocortical cultures with high concentrations of exogenous NO produces $ONOO^-$ and subsequent Zn(II) release from intracellular stores as visualized by Newport Green, TSQ, and RhodZin-3 (135). Temporary punctate fluorescence localized in the mitochondria occurred, suggesting that cytoplasmic Zn(II) may be taken up by mitochondria. Higher Zn(II) concentrations increased O_2^- production, resulting in mitochondrial dysfunction, additional $ONOO^-$ formation, and amplification of the signaling pathway. Nitric oxide–induced zinc release could be blocked by Mn(III) tetrakis(4-benzoic acid)porphyrin or superoxide dismutase both scavenge O_2^- and reduce $ONOO^-$ formation. These results suggest that $ONOO^-$, rather than NO alone, may be responsible for the observed action. The overproduction of $ONOO^-$ and reactive oxygen species can activate p38 mitogen-activated protein kinase, which in turn activates voltage-gated K^+ channels, resulting in cell volume loss and cell death. Zn(II) chelators, reactive oxygen species scavengers, or K^+ channel blockers all diminished NO-induced K^+ efflux and cell death. In similar studies, short-term exposure of cultured neurons to nonneurotoxic levels of NO resulted in a concentration-dependent increase in intracellular free Zn(II), measured by use

of FluoZin-3, without inducing cell death (136). These data suggest an important link between Zn(II) and NO in apoptotic signal transduction pathways.

In a study of the role of poly(ADP-ribose) polymerase (PARP) and poly(ADP-ribose) glycohydrolase (PARG) in zinc-mediated cell death, addition of 400 μM Zn(II) to cultured cortical cells resulted in an increase in PARP, with reduced levels of nicotinamide adenine dinucleotide (NAD) and ATP, resulting in cell death (137). Similarly, inhibition of the Zn-inducible enzyme NADPH oxidase and nNOS reduced Zn(II)-induced poly(ADP-ribosyl)ation. Upon exposure to Zn(II), NO levels in cortical cells increased as observed by DAF-FM fluorescence, which is consistent with increased **NOS** activity. This study showed that NADPH oxidase induction and nNOS contribute to PARP/PARG-mediated cell death induced by zinc.

3.2. Cardiovascular System

In rat aortic endothelial cells stained with Zinquin-E, addition of exogenous NO results in release of Zn(II) from MT. Increased fluorescence from Zinquin-E was observed in both the cytoplasm and nucleus (138). Pretreatment of cells with Zn(II) prior to Zinquin-E in the absence of an NO donor resulted in increased nuclear fluorescence, indicating that the fluorescence observed after NO treatment is not due to NO-mediated translocation of Zinquin to the nucleus but rather reflects Zn(II) nuclear content. Similar treatment of Zinquin-labeled mouse lung fibroblasts with NO donors showed increased labilization of zinc in wild type ($MT^{+/+}$) but not MT-deficient ($MT^{-/-}$) mutants (139). Moreover, studies in cultured endothelial cells from lung of wild-type and $MT^{-/-}$ mutants revealed that MT is vital in modulating the NO-induced change in zinc concentration in the pulmonary endothelium. Similar investigations in cultured pulmonary aortic cells also resulted in increased Zinquin fluorescence after treatment with NO donors. Overexpression of MT-I or coincubation with a zinc chelator protected mitochondria from NO/Zn-mediated apoptosis (140). Similarly, exposure of mouse lung endothelial cells to *S*-nitrosocysteine resulted in increased Zn(II)-induced fluorescence from Zinquin that could be removed by addition of the zinc chelator **TPEN**. No NO-mediated increase of labile Zn(II) was observed in MT-I or MT-II knockout mice, thus indicating the requirement of MT for the NO-mediated zinc release pathway. Pretreatment of sheep pulmonary artery endothelial cells (PAECs) with SNAP decreased the observed lipopolysaccharide (LPS)-induced apoptosis. Chelation of free zinc with TPEN reduced the protective effect of NO, thus suggesting that MT is the source of the labile zinc. Similarly, exposure of PAECs to NO donors resulted in an increase in free zinc, as observed by Zinquin fluorescence (141). Direct addition of $ZnCl_2$ to PAECs resulted in a dose-dependent increase in superoxide generation localized in the mitochondria. Overexpression of the zinc-binding protein MT-I or coincubation with TPEN protected the mitochondria from both NO- and zinc-mediated cell death.

Although NO generally has vasodilatory effects in the cardiovascular system, the NO/Zn(II) interplay has also been implicated in hypoxia-mediated NO biosynthesis that contributes to vasoconstriction. Under hypoxic conditions in **PAECs**, increased NO results in release of Zn(II) via nitrosation of **MT** and induces pulmonary vasoconstriction (142). Increases in endogenous NO were observed by the FRET construct cygnet-2 (130). MT-deficient ($MT^{-/-}$) mice displayed an 80% reduction in induced hypoxic pulmonary vasoconstriction. These studies indicate that hypoxia can induce NO production from PAECs and that the resultant increase in free zinc induces pulmonary vasoconstriction through a signaling cascade.

In isolated adult rat cardiomyocytes, NO mobilizes endogenous Zn(II) by opening mitochondrial K_{ATP} channels through the cGMP/PKG pathway. Zinc levels in such cells were monitored with Newport Green DCF (143). Addition of SNAP increases mobile zinc

levels, but this effect could be blocked by addition of inhibitors of sGC. PKG inhibition blocks the effects of SNAP, whereas addition of PKG activators in the absence of SNAP mimicked the effects of SNAP. In a similar pathway, morphine could mobilize intracellular Zn(II) by an NO-mediated pathway in rat cardiomyocytes (51). Treatment of the cardiomyocytes with morphine resulted in an increase in zinc as monitored by Newport Green. This effect was attenuated with L-N^G-nitroarginine methyl ester, an NO-synthase inhibitor, suggesting that the increase in Zn(II) was mediated by NO. Similarly, treatment with an sGC inhibitor prevented the morphine-dependent zinc release. Similar PKG inhibition was observed and NO was detected by DAF-FM. Morphine mobilized intracellular Zn by the NO/cGMP/PKG pathway and inhibited a mitochondrial permeability transition pore opening by inactivation of GSK-3β.

3.3. Immune System

Both zinc and nitric oxide participate in processes orchestrated by the immune system to defend against pathogens. Zinc deficiency leads to impaired immune function and increased susceptibility to infection (144). Exposure to endotoxins, such as proinflammatory cytokines and/or LPS, prompts expression of the iNOS and hence increased NO production under inflammatory conditions (145). A correlated action of the two inorganic species is featured within several signaling pathways in immune cells and immunologically active organs, such as skin, heart, and lung.

In cultured murine keratinocytes during cytokine-induced inflammation, the presence of 10 μM Zn(II) decreased NO production, a result of iNOS inhibition confirmed both at the protein and mRNA levels (146). Similarly, in ex vivo measurements on lung homogenates from LPS-treated rats, 150-μM Zn(II) concentrations inhibited iNOS activity (147). The influence of increased zinc concentrations on NO production is consistent with the anti-inflammatory activity of the ion and with the adverse effects of zinc deficiency on the immune system. Conversely, iNOS-derived NO affects intracellular zinc homeostasis in cytokine-activated murine aortic endothelial cells (148). Following iNOS induction during an inflammatory response, MT participates in transient release of intracellular zinc in the nuclei, where it is observed by fluorescence microscopy as a punctate pattern after staining with Zinquin. Although collected on different cell types, the foregoing data indicate a potential feedback loop that links the transient concentrations of zinc and nitric oxide during cellular response to inflammatory stimuli.

Zinc is also involved in the activation of microglia, the resident immune cells of the central nervous system. The activation of cultured microglia is triggered by zinc through the sequential activation of NADPH oxidase, poly(ADP-ribose)polymerase-1 and NF-κB (149). This finding was confirmed in ex vivo measurements on mouse brain after direct injection of $ZnCl_2$. Nitrite measurements using the Griess assay indicated an increase in NO production following zinc-induced microglial activation, an observation consistent with an immunological response yet in contrast with the typical anti-inflammatory effect of zinc. In the brain, where zinc is abundant relative to other organs and the neuronal isoform of NO synthase is an additional source of NO, the interplay of NO and Zn in the immune response may overlap with other phenomena involved in the neurobiology of these species, providing an as yet unexplored contribution to neurological pathology.

SUMMARY POINTS

1. Available turn-on sensors for biologically mobile zinc offer excellent methods for visualizing this ion with high spatial and temporal resolution. Sensors with a wide range of affinities for mobile zinc can be selected based on the specific application.

2. Strategies such as ratiometric imaging or specific sensor localization provide the opportunity for sophisticated experiments involving zinc quantification or localization with high subcellular resolution that can overcome the limitations of optical microscopy. The development of detection systems of this nature is still in its early stages.
3. Bright fluorescent probes for nitric oxide are available based on reactions of *o*-diamines with NO under aerobic conditions. Platforms incorporating fluorescein, rhodamine, and BODIPY dyes with a variety of absorption and emission wavelengths as well as cellular uptake characteristics are available for different applications.
4. Metal-based fluorescent indicators for nitric oxide based on Cu(II)-mediated *N*-nitrosation of amines incorporate probes that react directly with NO. Such constructs do not require oxygen for emission enhancement, making them ideal for hypoxic environments.
5. Fluorescent probes for biological zinc and nitric oxide reveal multiple pathways in which these inorganic species are interconnected in biology. Zn/NO synergism in the neuronal, cardiovascular, and immune systems have all benefited from such probes.

FUTURE ISSUES

1. The fields of zinc and nitric oxide sensing will profit from the development of more sensitive and selective probes that provide in a palette of colors to facilitate study of problems in which the concentration range of the analyte can vary.
2. Quantification of intracellular zinc is an important goal in devising new zinc probes. This task will require a toolbox of ratiometric probes that span a wide range of zinc affinities with large dynamic ranges.
3. Fluorescent probes able to detect nitric oxide reversibly are much desired. Solutions to this problem may arise from the use of nitric oxide to modulate inherently reversible interactions, such as formation of metal nitrosyls or mediation of conformational changes.
4. A complete network map of the temporal, positional, and functional properties of nitric oxide will require specific probes for downstream NO oxidation products and other reactive nitrogen/oxygen species. Such probes should be highly selective and report endogenous levels of these analytes. Differentiating NO transfer agents, such as *S*-nitrosothiols, from nitric oxide will require creative chemistry.
5. Much additional work to elucidate the biological interplay between these two important endogenous analytes can be garnered by using NO and Zn probes concomitantly. Such experiments will require the use of probes that are compatible, different in color, and specifically distributed in cells.
6. The utilization of site-specific probes anchored to cellular compartments will enhance the topological resolution of fluorescence detection. Protein design and protein labeling methodologies will continue to supply powerful strategies for site-specific sensor design.
7. Use of other imaging techniques, such as magnetic resonance imaging, can complement fluorescence imaging techniques. Sensors with dual fluorescence and magnetic resonance imaging modalities will be particularly useful for monitoring NO and Zn at different concentrations or tissue depths.

Acknowledgments

This work was supported by grants from the National Science Foundation (CHE-0907905 to S.J.L.) and the National Institutes of Health (GM065519 to S.J.L., K99GM092970 to M.D.P.). The content is solely the responsibility of the authors and does not necessarily represent the official views of the National Institute of General Medical Sciences or the National Institutes of Health.

LITERATURE CITED

1. Andreini C, Banci L, Bertini I, Rosato A. Counting the zinc-proteins encoded in the human genome. J. Proteome Res. 2006; 5:196–201. [PubMed: 16396512]
2. Sousa SF, Lopes AB, Fernandes PA, Ramos MJ. The zinc proteome: a tale of stability and functionality. Dalton Trans. 2009; (38):7946–7956. [PubMed: 19771357]
3. Maret W, Li Y. Coordination dynamics of zinc in proteins. Chem. Rev. 2009; 109:4682–4707. [PubMed: 19728700]
4. Lichten LA, Cousins RJ. Mammalian zinc transporters: nutritional and physiologic regulation. Annu. Rev. Nutr. 2009; 29:153–176. [PubMed: 19400752]
5. Maret W. The function of zinc metallothionein: a link between cellular zinc and redox state. J. Nutr. 2000; 130:S1455–S1458.
6. Vallee BL, Falchuk KH. The biochemical basis of zinc physiology. Physiol. Rev. 1993; 73:79–118. [PubMed: 8419966]
7. Maret W, Krężel A. Cellular zinc and redox buffering capacity of metallothionein/thionein in health and disease. Mol. Med. 2007; 13:371–375. [PubMed: 17622324]
8. Frederickson CJ, Koh J-Y, Bush AI. The neurobiology of zinc in health and disease. Nat. Rev. Neurosci. 2005; 6:449–462. [PubMed: 15891778]
9. Takeda A, Tamano H. Insight into zinc signaling from dietary zinc deficiency. Brain Res. Rev. 2009; 62:33–44. [PubMed: 19747942]
10. Kay AR, Tóth K. Is zinc a neuromodulator? Sci. Signal. 2008; 1:re3. [PubMed: 18480018]
11. Sensi SL, Paoletti P, Bush AI, Sekler I. Zinc in the physiology and pathology of the CNS. Nat. Rev. Neurosci. 2009; 10:780–791. [PubMed: 19826435]
12. Taylor CG. Zinc, the pancreas, and diabetes: insights from rodent studies and future directions. BioMetals. 2005; 18:305–312. [PubMed: 16158221]
13. Jansen J, Karges W, Rink L. Zinc and diabetes-clinical links and molecular mechanisms. J. Nutr. Biochem. 2009; 20:399–417. [PubMed: 19442898]
14. Wijesekara N, Chimienti F, Wheeler MB. Zinc, a regulator of islet function and glucose homeostasis. Diabetes Obes. Metab. 2009; 11:202–214. [PubMed: 19817803]
15. Costello LC, Franklin RB. The clinical relevance of the metabolism of prostate cancer; zinc and tumor suppression: connecting the dots. Mol. Cancer. 2006; 5:17. [PubMed: 16700911]
16. Franklin RB, Costello LC. Zinc as an antitumor agent in prostate cancer and in other cancers. Arch. Biochem. Biophys. 2007; 463:211–217. [PubMed: 17400177]
17. Costello LC, Franklin RB. Prostatic fluid electrolyte composition for the screening of prostate cancer: apotential solution to a major problem. Prostate Cancer Prostatic Dis. 2009; 12:17–24. [PubMed: 18591961]
18. Ghosh SK, Kim P, Zhang X-A, Yun S-H, Moore A, et al. A novel imaging approach for early detection of prostate cancer based on endogenous zinc sensing. Cancer Res. 2010; 70:6119–6127. [PubMed: 20610630]
19. Ignarro LJ, Buga GM, Wood KS, Byrns RE, Chaudhuri G. Endothelium-derived relaxing factor produced and released from artery and vein is nitric oxide. Proc. Natl. Acad. Sci. USA. 1987; 84:9265–9269. [PubMed: 2827174]
20. Palmer RMJ, Ferrige AG, Moncada S. Nitric oxide release accounts for the biological activity of endothelium-derived relaxing factor. Nature. 1987; 327:524–526. [PubMed: 3495737]
21. Marletta MA, Yoon PS, Iyengar R, Leaf CD, Wishnok JS. Macrophage oxidation of L-arginine to nitrite and nitrate: Nitric oxide is an intermediate. Biochemistry. 1988; 27:8706–8711. [PubMed: 3242600]

22. Bredt DS, Hwang PM, Snyder SH. Localization of nitric oxide synthase indicating a neural role for nitric oxide. Nature. 1990; 347:768–770. [PubMed: 1700301]
23. Shibuki K, Okada D. Endogenous nitric oxide release required for long-term synaptic depression in the cerebellum. Nature. 1991; 349:326–328. [PubMed: 1702879]
24. Loscalzo J, Welch G. Nitric oxide and its role in the cardiovascular system. Prog. Cardiovasc. Dis. 1995; 38:87–104. [PubMed: 7568906]
25. Bogdan C. Nitric oxide and the immune response. Nat. Immunol. 2001; 2:907–916. [PubMed: 11577346]
26. Fukumura D, Kashiwagi S, Jain RK. The role of nitric oxide in tumour progression. Nat. Rev. Cancer. 2006; 6:521–534. [PubMed: 16794635]
27. Garthwaite J. Concepts of neural nitric oxide--mediated transmission. Eur. J. Neurosci. 2008; 27:2783–2802. [PubMed: 18588525]
28. Gladwin MT, Schechter AN, Kim-Shapiro DB, Patel RP, Hogg N, et al. The emerging biology of the nitrite anion. Nat. Chem. Biol. 2005; 1:308–314. [PubMed: 16408064]
29. Bryan NS. Nitrite in nitric oxide biology: Cause or consequence? A systems-based review. Free Radic. Biol. Med. 2006; 41:691–701. [PubMed: 16895789]
30. Johnson RA, Freeman RH. Sustained hypertension in the rat induced by chronic blockade of nitric oxide production. Am. J. Hypertens. 1992; 5:919–922. [PubMed: 1285942]
31. Weis M, Kledal TN, Lin KY, Panchal SN, Gao SZ, et al. Cytomegalovirus infection impairs the nitric oxide synthase pathway: role of asymmetric dimethylarginine in transplant arteriosclerosis. Circulation. 2004; 109:500–505. [PubMed: 14732750]
32. Rajfer J, Aronson WJ, Bush PA, Dorey FJ, Ignarro LJ. Nitric oxide as a mediator of relaxation of the corpus cavernosum in response to nonadrenergic, noncholinergic neurotransmission. N. Engl. J. Med. 1992; 326:90–94. [PubMed: 1309211]
33. Pieper GM. Review of alterations in endothelial nitric oxide production in diabetes: protective role of arginine on endothelial dysfunction. Hypertension. 1998; 31:1047–1060. [PubMed: 9576113]
34. Oyadomari S, Takeda K, Takiguchi M, Gotoh T, Matsumoto M, et al. Nitric oxide--induced apoptosis in pancreatic β cells is mediated by the endoplasmic reticulum stress pathway. Proc. Natl. Acad. Sci. USA. 2001; 98:10845–10850. [PubMed: 11526215]
35. Chan PH. Reactive oxygen radicals in signaling and damage in the ischemic brain. J. Cereb. Blood Flow Metab. 2001; 21:2–14. [PubMed: 11149664]
36. Titheradge MA. Nitric oxide in septic shock. Biochim. Biophys. Acta. 1999; 1411:437–455. [PubMed: 10320674]
37. Smith KJ, Lassmann H. The role of nitric oxide in multiple sclerosis. Lancet Neurol. 2002; 1:232–241. [PubMed: 12849456]
38. Hussain SP, Hofseth LJ, Harris CC. Radical causes of cancer. Nat. Rev. Cancer. 2003; 3:276–285. [PubMed: 12671666]
39. Heales SJR, Bolaños JP, Stewart VC, Brookes PS, Land JM, Clark JB. Nitric oxide, mitochondria and neurological disease. Biochim. Biophys. Acta. 1999; 1410:215–228. [PubMed: 10076028]
40. Brown GC, Bal-Price A. Inflammatory neurodegeneration mediated by nitric oxide, glutamate, and mitochondria. Mol. Neurobiol. 2003; 27:325–355. [PubMed: 12845153]
41. Fukuto JM, Dutton AS, Houk KN. The chemistry and biology of nitroxyl (HNO): a chemically unique species with novel and important biological activity. ChemBioChem. 2005; 6:612–619. [PubMed: 15619720]
42. Szabó C, Ischiropoulos H, Radi R. Peroxynitrite: biochemistry, pathophysiology and development of therapeutics. Nat. Rev. Drug Discov. 2007; 6:662–680. [PubMed: 17667957]
43. Kikuchi K, Komatsu K, Nagano T. Zinc sensing for cellular application. Curr. Opin. Chem. Biol. 2004; 8:182–191. [PubMed: 15062780]
44. Jiang P, Guo Z. Fluorescent detection of zinc in biological systems: recent development on the design of chemosensors and biosensors. Coord. Chem. Rev. 2004; 248:205–229.
45. Carol P, Sreejith S, Ajayaghosh A. Ratiometric and near-infrared molecular probes for the detection and imaging of zinc ions. Chem. Asian J. 2007; 2:338–348. [PubMed: 17441169]

46. Domaille DW, Que EL, Chang CJ. Synthetic fluorescent sensors for studying the cell biology of metals. Nat. Chem. Biol. 2008; 4:168–175. [PubMed: 18277978]
47. McRae R, Bagchi P, Sumalekshmy S, Fahrni CJ. In situ imaging of metals in cells and tissues. Chem. Rev. 2009; 109:4780–4827. [PubMed: 19772288]
48. Nolan EM, Lippard SJ. Small-molecule fluorescent sensors for investigating zinc metalloneurochemistry. Acc. Chem. Res. 2009; 42:193–203. [PubMed: 18989940]
49. Tomat E, Lippard SJ. Imaging mobile zinc in biology. Curr. Opin. Chem. Biol. 2010; 14:225–230. [PubMed: 20097117]
50. Vinkenborg JL, Koay MS, Merkx M. Fluorescent imaging of transition metal homeostasis using genetically encoded sensors. Curr. Opin. Chem. Biol. 2010; 14:231–237. [PubMed: 20036601]
51. Xi JK, Tian W, Zhang L, Jin YL, Xu ZL. Morphine prevents the mitochondrial permeability transition pore opening through NO/cGMP/PKG/Zn^{2+}/GSK-3β signal pathway in cardiomyocytes. Am. J. Physiol. Heart Circ. Physiol. 2009; 298:H601–H607. [PubMed: 19966058]
52. Ghafourifar, P.; Parihar, MS.; Nazarewicz, R.; Zenebe, WJ.; Parihar, A. Nitric oxide, part F: Oxidative and nitrosative stress in redox regulation of cell signaling. 2008. p. 317-334.
53. Gomes A, Fernandes E, Lima JLFC. Use of fluorescence probes for detection of reactive nitrogen species: a review. J. Fluoresc. 2006; 16:119–139. [PubMed: 16477509]
54. Hetrick EM, Schoenfisch MH. Analytical chemistry of nitric oxide. Annu. Rev. Anal. Chem. 2009; 2:409–433.
55. Hong H, Sun J, Cai W. Multimodality imaging of nitric oxide and nitric oxide synthases. Free Radic. Biol. Med. 2009; 47:684–698. [PubMed: 19524664]
56. McQuade LE, Lippard SJ. Fluorescent probes to investigate nitric oxide and other reactive nitrogen species in biology. Curr. Opin. Chem. Biol. 2010; 14:43–49. [PubMed: 19926519]
57. Nagano T. Bioimaging probes for reactive oxygen species and reactive nitrogen species. J. Clin. Biochem. Nutr. 2009; 45:111–124. [PubMed: 19794917]
58. Nagano T, Yoshimura T. Bioimaging of nitric oxide. Chem. Rev. 2002; 102:1235–1269. [PubMed: 11942795]
59. Wardman P. Fluorescent and luminescent probes for measurement of oxidative and nitrosative species in cells and tissues: progress, pitfalls, and prospects. Free Radic. Biol. Med. 2007; 43:995–1022. [PubMed: 17761297]
60. Ye X, Rubakhin SS, Sweedler JV. Detection of nitric oxide in single cells. Analyst. 2008; 133:423–433. [PubMed: 18365109]
61. Mahanand D, Houck JC. Fluorometric determination of zinc in biologic fluids. Clin. Chem. 1968; 14:6–11.
62. Smith GL, Jenkins RA, Gough JF. A fluorescent method for the detection and localization of zinc in human granulocytes. J. Histochem. Cytochem. 1969; 17:749–750. [PubMed: 5386301]
63. Frederickson CJ, Kasarskis EJ, Ringo D, Frederickson RE. A quinoline fluorescence method for visualizing and assaying the histochemically reactive zinc (bouton zinc) in the brain. J. Neurosci. Methods. 1987; 20:91–103. [PubMed: 3600033]
64. Zalewski PD, Millard SH, Forbes IJ, Kapaniris O, Slavotinek A, et al. Video image analysis of labile zinc in viable pancreatic islet cells using a specific fluorescent probe for zinc. J. Histochem. Cytochem. 1994; 42:877–884. [PubMed: 8014471]
65. Fahrni CJ, O'Halloran TV. Aqueous coordination chemistry of quinoline-based fluorescence probes for the biological chemistry of zinc. J. Am. Chem. Soc. 1999; 121:11448–11458.
66. Burdette SC, Walkup GK, Spingler B, Tsien RY, Lippard SJ. Fluorescent sensors for Zn^{2+} based on a fluorescein platform: synthesis, properties and intracellular distribution. J. Am. Chem. Soc. 2001; 123:7831–7841. [PubMed: 11493056]
67. Wong BA, Friedle S, Lippard SJ. Solution and fluorescence properties of symmetric dipicolylamine-containing dichlorofluorescein-based Zn^{2+} sensors. J. Am. Chem. Soc. 2009; 131:7142–7152. [PubMed: 19405465]
68. Xu Z, Yoon J, Spring DR. Fluorescent chemosensors for Zn^{2+} Chem. Soc. Rev. 2010; 39:1996–2006. [PubMed: 20428518]

69. Nolan EM, Ryu JW, Jaworski J, Feazell RP, Sheng M, Lippard SJ. Zinspy sensors with enhanced dynamic range for imaging neuronal cell zinc uptake and mobilization. J. Am. Chem. Soc. 2006; 128:15517–15528. [PubMed: 17132019]
70. Nolan EM, Jaworski J, Okamoto K-I, Hayashi Y, Sheng M, Lippard SJ. QZ1 and QZ2: rapid, reversible quinoline-derivatized fluoresceins for sensing biological Zn(II). J. Am. Chem. Soc. 2005; 127:16812–16823. [PubMed: 16316228]
71. Zhang X-A, Hayes D, Smith SJ, Friedle S, Lippard SJ. New strategy for quantifying biological zinc by a modified Zinpyr fluorescence sensor. J. Am. Chem. Soc. 2008; 130:15788–15789. [PubMed: 18975868]
72. Hirano T, Kikuchi K, Urano Y, Higuchi T, Nagano T. Highly zinc-selective fluorescent sensor molecules suitable for biological applications. J. Am. Chem. Soc. 2000; 122:12399–12400.
73. Komatsu K, Kikuchi K, Kojima H, Urano Y, Nagano T. Selective zinc sensor molecules with various affinities for Zn^{2+}, revealing dynamics and regional distribution of synaptically released Zn^{2+} in hippocampal slices. J. Am. Chem. Soc. 2005; 127:10197–10204. [PubMed: 16028930]
74. Haugland, RP. Handbook of Fluorescent Probes and Research Products. Eugene, OR: Molecular Probes; 2002. p. 919
75. Xu Z, Baek K-H, Kim HN, Cui J, Qian X, et al. Zn^{2+}-triggered amide tautomerization produces a highly Zn^{2+}-selective, cell-permeable, and ratiometric fluorescent sensor. J. Am. Chem. Soc. 2009; 132:601–610. [PubMed: 20000765]
76. Gee KR, Zhou Z-L, Qian W-J, Kennedy R. Detection and imaging of zinc secretion from pancreatic β-cells using a new fluorescent zinc indicator. J. Am. Chem. Soc. 2002; 124:776–778. [PubMed: 11817952]
77. Zhao J, Bertoglio BA, Gee KR, Kay AR. The zinc indicator FluoZin-3 is not perturbed significantly by physiological levels of calcium or magnesium. Cell Calcium. 2008; 44:422–426. [PubMed: 18353435]
78. Komatsu K, Urano Y, Kojima H, Nagano T. Development of an minocoumarin-based zinc sensor suitable for ratiometric fluorescence imaging of neuronal zinc. J. Am. Chem. Soc. 2007; 129:13447–13454. [PubMed: 17927174]
79. Han Z-X, Zhang X-B, Li Z, Gong Y-J, Wu X-Y, et al. Efficient fluorescence resonance energy transfer-based ratiometric fluorescent cellular imaging probe for Zn^{2+} using a rhodamine spirolactam as a trigger. Anal. Chem. 2010; 82:3108–3113. [PubMed: 20334436]
80. Dittmer PJ, Miranda JG, Gorski JA, Palmer AE. Genetically encoded sensors to elucidate spatial distribution of cellular zinc. J. Biol. Chem. 2009; 284:16289–16297. [PubMed: 19363034]
81. Vinkenborg JL, Nicolson TJ, Bellomo EA, Koay MS, Rutter GA, Merkx M. Genetically encoded FRET sensors to monitor intracellular Zn^{2+} homeostasis. Nat. Methods. 2009; 6:737–740. [PubMed: 19718032]
82. Marks KM, Nolan GP. Chemical labeling strategies for cell biology. Nat. Methods. 2006; 3:591–596. [PubMed: 16862131]
83. Johnsson N, Johnsson K. Chemical tools for biomolecular imaging. ACS Chem. Biol. 2007; 2:31–38. [PubMed: 17243781]
84. Keppler A, Gendreizig S, Gronemeyer T, Pick H, Vogel H, Johnsson K. A general method for the covalent labeling of fusion proteins with small molecules in vivo. Nat. Biotechnol. 2003; 21:86–89. [PubMed: 12469133]
85. Tomat E, Nolan EM, Jaworski J, Lippard SJ. Organelle-specific zinc detection using Zinpyr-labeled fusion proteins in live cells. J. Am. Chem. Soc. 2008; 130:15776–15777. [PubMed: 18973293]
86. Hornig FS, Korth H-G, Rauen U, de Groot H, Sustmann R. Synthesis and properties of a pH-insensitive fluorescent nitric oxide cheletropic trap (FNOCT). Helv. Chim. Acta. 2006; 89:2281–2296.
87. Meineke P, Rauen U, de Groot H, Korth HG, Sustmann R. Nitric oxide detection and visualization in biological systems. Applications of the FNOCT method. Biol. Chem. 2000; 381:575–582. [PubMed: 10987364]

88. Meineke P, Rauen U, de Groot H, Korth H-G, Sustmann R. Cheletropic traps for the fluorescence spectroscopic detection of nitric oxide (nitrogen monoxide) in biological systems. Chem. Eur. J. 1999; 5:1738–1747.

89. Green LC, Wagner DA, Glogowski J, Skipper PL, Wishnok JS, Tannenbaum SR. Analysis of nitrate, nitrite, and [N-15]-labeled nitrate in biological-fluids. Anal. Biochem. 1982; 126:131–138. [PubMed: 7181105]

90. Griess P. Bemerkungen zu der abhandlung der HH. Weselky und benedikt ueber einige azoverbindungen. Ber. Dtsch. Chem. Ges. 1879; 12:426–428.

91. Nagano T, Takizawa H, Hirobe M. Reactions of nitric oxide with amines in the presence of dioxygen. Tetrahedron Lett. 1995; 36:8239–8242.

92. Misko TP, Schilling RJ, Salvemini D, Moore WM, Currie MG. A fluorometric assay for the measurement of nitrite in biological samples. Anal. Biochem. 1993; 214:11–16. [PubMed: 7504409]

93. Marzinzig M, Nussler AK, Stadler J, Marzinzig E, Barthlen W, et al. Improved methods to measure end products of nitric oxide in biological fluids: nitrite, nitrate, and *S*-nitrosothiols. Nitric Oxide. 1997; 1:177–189. [PubMed: 9701056]

94. Kojima H, Nakatsubo N, Kikuchi K, Urano Y, Higuchi T, et al. Direct evidence of NO production in rat hippocampus and cortex using a new fluorescent indicator: DAF-2 DA. NeuroReport. 1998; 9:3345–3348. [PubMed: 9855277]

95. Kojima H, Nakatsubo N, Kikuchi K, Kawahara S, Kirino Y, et al. Detection and imaging of nitric oxide with novel fluorescent indicators: diaminofluoresceins. Anal. Chem. 1998; 70:2446–2453. [PubMed: 9666719]

96. Nakatsubo N, Kojima H, Kikuchi K, Nagoshi H, Hirata Y, et al. Direct evidence of nitric oxide production from bovine aortic endothelial cells using new fluorescence indicators: diaminofluoresceins. FEBS Lett. 1998; 427:263–266. [PubMed: 9607324]

97. Kim W-S, Ye XY, Rubakhin SS, Sweedler JV. Measuring nitric oxide in single neurons by capillary electrophoresis with laser-induced fluorescence: use of ascorbate oxidase in diaminofluorescein measurements. Anal. Chem. 2006; 78:1859–1865. [PubMed: 16536421]

98. Broillet M-C, Randin O, Chatton J-Y. Photoactivation and calcium sensitivity of the fluorescent NO indicator 4,5-diaminofluorescein (DAF-2): implications for cellular NO imaging. FEBS Lett. 2001; 491:227–232. [PubMed: 11240132]

99. Kojima H, Urano Y, Kikuchi K, Higuchi T, Hirata Y, Nagano T. Fluorescent indicators for imaging nitric oxide production. Angew. Chem. Int. Ed. Engl. 1999; 38:3209–3212. [PubMed: 10556905]

100. Kojima H, Hirotani M, Nakatsubo N, Kikuchi K, Urano Y, et al. Bioimaging of nitric oxide with fluorescent indicators based on the rhodamine chromophore. Anal. Chem. 2001; 73:1967–1973. [PubMed: 11354477]

101. Heiduschka P, Thanos S. NO production during neuronal cell death can be directly assessed by a chemical reaction in vivo. NeuroReport. 1998; 9:4051–4057. [PubMed: 9926846]

102. Galindo F, Kabir N, Gavrilovic J, Russell DA. Spectroscopic studies of 1,2-diaminoanthraquinone (DAQ) as a fluorescent probe for the imaging of nitric oxide in living cells. Photochem. Photobiol. Sci. 2008; 7:126–130. [PubMed: 18167606]

103. Gabe Y, Ueno T, Urano Y, Kojima H, Nagano T. Tunable design strategy for fluorescence probes based on 4-substituted BODIPY chromophore: improvement of highly sensitive fluorescence probe for nitric oxide. Anal. Bioanal. Chem. 2006; 386:621–626. [PubMed: 16924384]

104. Gabe Y, Urano Y, Kikuchi K, Kojima H, Nagano T. Highly sensitive fluorescence probes for nitric oxide based on boron dipyrromethene chromophore-rational design of potentially useful bioimaging fluorescence probe. J. Am. Chem. Soc. 2004; 126:3357–3367. [PubMed: 15012166]

105. Sasaki E, Kojima H, Nishimatsu H, Urano Y, Kikuchi K, et al. Highly sensitive near-infrared fluorescent probes for nitric oxide and their application to isolated organs. J. Am. Chem. Soc. 2005; 127:3684–3685. [PubMed: 15771488]

106. Izumi S, Urano Y, Hanaoka K, Terai T, Nagano T. A simple and effective strategy to increase the sensitivity of fluorescence probes in living cells. J. Am. Chem. Soc. 2009; 131:10189–10200. [PubMed: 19572714]

107. Zhang R, Ye Z, Wang G, Zhang W, Yuan J. Development of a ruthenium(II) complex based luminescent probe for imaging nitric oxide production in living cells. Chem. Eur. J. 2010; 16:6884–6891. [PubMed: 20458707]
108. Kim JH, Heller DA, Jin H, Barone PW, Song C, et al. The rational design of nitric oxide selectivity in single-walled carbon nanotube near-infrared fluorescence sensors for biological detection. Nat. Chem. 2009; 1:473–481. [PubMed: 21378915]
109. Yang Y, Seidlits SK, Adams MM, Lynch VM, Schmidt CE, et al. A highly selective low-background fluorescent imaging agent for nitric oxide. J. Am. Chem. Soc. 2010; 132:13114–13116. [PubMed: 20672823]
110. Lim MH, Xu D, Lippard SJ. Visualization of nitric oxide in living cells by a copper-based fluorescent probe. Nat. Chem. Biol. 2006; 2:375–380. [PubMed: 16732295]
111. Lim MH, Wong BA, Pitcock WH, Mokshagundam D, Baik MH, Lippard SJ. Direct nitric oxide detection in aqueous solution by copper(II) fluorescein complexes. J. Am. Chem. Soc. 2006; 128:14364–14373. [PubMed: 17076510]
112. Lim MH, Lippard SJ. Metal-based turn-on fluorescent probes for sensing nitric oxide. Acc. Chem. Res. 2007; 40:41–51. [PubMed: 17226944]
113. McQuade LE, Pluth MD, Lippard SJ. Mechanism of nitric oxide reactivity and fluorescence enhancement of the NO-specific probe, CuFL1. Inorg. Chem. 2010; 49:8025–8033. [PubMed: 20704359]
114. Gusarov I, Starodubtseva M, Wang ZQ, McQuade L, Lippard SJ, et al. Bacterial nitric-oxide synthases operate without a dedicated redox partner. J. Biol. Chem. 2008; 283:13140–13147. [PubMed: 18316370]
115. Shatalin K, Gusarov I, Avetissova E, Shatalina Y, McQuade LE, et al. *Bacillus anthracis*-derived nitric oxide is essential for pathogen virulence and survival in macrophages. Proc. Natl. Acad. Sci. USA. 2008; 105:1009–1013. [PubMed: 18215992]
116. McQuade LE, Lippard SJ. Fluorescence-based nitric oxide sensing by Cu(II) complexes that can be trapped in living cells. Inorg. Chem. 2010; 49:7464–7471. [PubMed: 20690755]
117. McQuade LE, Ma J, Lowe G, Ghatpande A, Gelperin A, Lippard SJ. Visualization of nitric oxide production in the mouse main olfactory bulb by a cell-trappable copper(II) fluorescent probe. Proc. Natl. Acad. Sci. USA. 2010; 107:8525–8530. [PubMed: 20413724]
118. Ouyang J, Hong H, Shen C, Zhao Y, Ouyang CG, et al. A novel fluorescent probe for the detection of nitric oxide in vitro and in vivo. Free Radic. Biol. Med. 2008; 45:1426–1436. [PubMed: 18804530]
119. Ortiz M, Torréns M, Mola JL, Ortiz PJ, Fragoso A, et al. Nitric oxide binding and photodelivery based on ruthenium(II) complexes of 4-arylazo-3,5-dimethylpyrazole. Dalton Trans. 2008; 27:3559–3566. [PubMed: 18594704]
120. Soh N, Katayama Y, Maeda M. A fluorescent probe for monitoring nitric oxide production using a novel detection concept. Analyst. 2001; 126:564–566. [PubMed: 11394293]
121. Katayama Y, Takahashi S, Maeda M. Design, synthesis and characterization of a novel fluorescent probe for nitric oxide (nitrogen monoxide). Anal. Chim. Acta. 1998; 365:159–167.
122. Lim MH, Lippard SJ. Fluorescence-based nitric oxide detection by ruthenium porphyrin fluorophore complexes. Inorg. Chem. 2004; 43:6366–6370. [PubMed: 15446885]
123. Hilderbrand SA, Lim MH, Lippard SJ. Dirhodium tetracarboxylate scaffolds as reversible fluorescence-based nitric oxide sensors. J. Am. Chem. Soc. 2004; 126:4972–4978. [PubMed: 15080703]
124. Eroy-Reveles AA, Mascharak PK. Nitric oxide--donating materials and their potential in pharmacological applications for site-specific nitric oxide delivery. Future Med. Chem. 2009; 1:1497–1507. [PubMed: 21426062]
125. Patra AK, Rose MJ, Murphy KA, Olmstead MM, Mascharak PK. Photolabile ruthenium nitrosyls with planar dicarboxamide tetradentate N4 ligands: effects of in-plane and axial ligand strength on NO release. Inorg. Chem. 2004; 43:4487–4495. [PubMed: 15236563]
126. Patra AK, Afshar R, Olmstead MM, Mascharak PK. The first non-heme iron(III) complex with a ligated carboxamido group that exhibits photolability of a bound NO ligand. Angew. Chem. Int. Ed. 2002; 41:2512–2515.

127. Pearce LL, Gandley RE, Han WP, Wasserloos K, Stitt M, et al. Role of metallothionein in nitric oxide signaling as revealed by a green fluorescent fusion protein. Proc. Natl. Acad. Sci. USA. 2000; 97:477–482. [PubMed: 10618443]
128. Barker SLR, Clark HA, Swallen SF, Kopelman R, Tsang AW, Swanson JA. Ratiometric and fluorescence-lifetime-based biosensors incorporating cytochrome c' and the detection of extra- and intracellular macrophage nitric oxide. Anal. Chem. 1999; 71:1767–1772. [PubMed: 10330907]
129. Barker SLR, Zhao YD, Marletta MA, Kopelman R. Cellular applications of a sensitive and selective fiber-optic nitric oxide biosensor based on a dye-labeled heme domain of soluble guanylate cyclase. Anal. Chem. 1999; 71:2071–2075. [PubMed: 10366889]
130. Honda A, Adams SR, Sawyer CL, Lev-Ram V, Tsien RY, Dostmann WRG. Spatiotemporal dynamics of guanosine $3',5'$-cyclic monophosphate revealed by a genetically encoded, fluorescent indicator. Proc. Natl. Acad. Sci. USA. 2001; 98:2437–2442. [PubMed: 11226257]
131. Sato M, Nakajima T, Goto M, Umezawa Y. Cell-based indicator to visualize picomolar dynamics of nitric oxide release from living cells. Anal. Chem. 2006; 78:8175–8182. [PubMed: 17165805]
132. Sato M, Hida N, Umezawa Y. Imaging the nanomolar range of nitric oxide with an amplifier-coupled fluorescent indicator in living cells. Proc. Natl. Acad. Sci. USA. 2005; 102:14515–14520. [PubMed: 16176986]
133. Sato M, Hida N, Ozawa T, Umezawa Y. Fluorescent indicators for cyclic GMP based on cyclic GMP-dependent protein kinase I and green fluorescent proteins. Anal. Chem. 2000; 72:5918–5924. [PubMed: 11140757]
134. Cuajungco MP, Lees GJ. Nitric oxide generators produce accumulation of chelatable zinc in hippocampal neuronal perikarya. Brain Res. 1998; 799:118–129. [PubMed: 9666098]
135. Bossy-Wetzel E, Talantova MV, Lee WD, Scholzke MN, Harrop A, et al. Crosstalk between nitric oxide and zinc pathways to neuronal cell death involving mitochondrial dysfunction and p38-activated K^+ channels. Neuron. 2004; 41:351–365. [PubMed: 14766175]
136. Lin W, Mohandas B, Fontaine CP, Colvin RA. Release of intracellular Zn^{2+} in cultured neurons after brief exposure to low concentrations of exogenous nitric oxide. BioMetals. 2007; 20:891–901. [PubMed: 17279325]
137. Kim YH, Koh JY. The role of NADPH oxidase and neuronal nitric oxide synthase in zinc-induced poly(ADP-ribose) polymerase activation and cell death in cortical culture. Exp. Neurol. 2002; 177:407–418. [PubMed: 12429187]
138. Berendji D, Kolb-Bachofen V, Meyer KL, Grapenthin O, Weber H, et al. Nitric oxide mediates intracytoplasmic and intranuclear zinc release. FEBS Lett. 1997; 405:37–41. [PubMed: 9094420]
139. St Croix CM, Wasserloos KJ, Dineley KE, Reynolds IJ, Levitan ES, Pitt BR. Nitric oxide--induced changes in intracellular zinc homeostasis are mediated by metallothionein/thionein. Am. J. Physiol. Lung Cell. Mol. Physiol. 2002; 282:L185–L192. [PubMed: 11792622]
140. Tang Z-L, Wasserloos KJ, Liu XH, Stitt MS, Reynolds IJ, et al. Nitric oxide decreases the sensitivity of pulmonary endothelial cells to LPS-induced apoptosis in a zinc-dependent fashion. Mol. Cell. Biochem. 2002; 234:211–217. [PubMed: 12162436]
141. Wiseman DA, Wells SM, Wilham J, Hubbard M, Welker JE, Black SM. Endothelial response to stress from exogenous Zn^{2+} resembles that of NO-mediated nitrosative stress, and is protected by MT-1 overexpression. Am. J. Physiol. Cell Physiol. 2006; 291:C555–C568. [PubMed: 16723513]
142. Bernal PJ, Leelavanichkul K, Bauer E, Cao R, Wilson A, et al. Nitric oxide--mediated zinc release contributes to hypoxic regulation of pulmonary vascular tone. Circ. Res. 2008; 102:1575–1583. [PubMed: 18483408]
143. Jang Y, Wang H, Xi J, Mueller RA, Norfleet EA, Xu Z. NO mobilizes intracellular Zn^{2+} via cGMP/PKG signaling pathway and prevents mitochondrial oxidant damage in cardiomyocytes. Cardiovasc. Res. 2007; 75:426–433. [PubMed: 17570352]
144. Haase H, Rink L. Functional significance of zinc-related signaling pathways in immune cells. Annu. Rev. Nutr. 2009; 29:133–152. [PubMed: 19400701]
145. Pautz A, Art J, Hahn S, Nowag S, Voss C, Kleinert H. Regulation of the expression of inducible nitric oxide synthase. Nitric Oxide. 2010; 23:75–93. [PubMed: 20438856]

146. Yamaoka J, Kume T, Akaike A, Miyachi Y. Suppressive effect of zinc ion on iNOS expression induced by interferon-β or tumor necrosis factor-γ in murine keratinocytes. J. Dermatol. Sci. 2000; 23:27–35. [PubMed: 10699762]

147. Abou-Mohamed G, Papapetropoulos A, Catravas JD, Caldwell RW. Zn^{2+} inhibits nitric oxide formation in response to lipopolysaccharides: implication in its anti-inflammatory activity. Eur. J. Pharmacol. 1998; 341:265–272. [PubMed: 9543248]

148. Spahl DU, Berendji-Grün D, Suschek CV, Kolb-Bachofen V, Kröncke K-D. Regulation of zinc homeostasis by inducible NO synthase-derived NO: nuclear metallothionein translocation and intranuclear Zn^{2+} release. Proc. Natl. Acad. Sci. USA. 2003; 100:13952–13957. [PubMed: 14617770]

149. Kauppinen TM, Higashi Y, Suh SW, Escartin C, Nagasawa K, Swanson RA. Zinc triggers microglial activation. J. Neurosci. 2008; 28:5827–5835. [PubMed: 18509044]

TERMS/DEFINITIONS LIST

Förster (or fluorescence) resonance energy transfer (FRET)	This occurs between the excited state of a donor molecule (D) and the ground state of an acceptor molecule (A) through nonradiative dipole-dipole coupling. For fluorescent chromophores, emission from D overlaps with the absorption spectrum of A and results in emission from A at a longer wavelength. A common application of (F)RET is for distance measurement between two sites in macromolecules based on the D-A energy transfer efficiency.
Photoinduced-electron transfer (PET)	This occurs when higher-energy lone pair electrons (often from an amine nitrogen) quench the excited state of a fluorophore thus extinguishing or attenuating its emission. Following photoinduced excitation of a ground-state electron of the fluorophore, the lone pair electrons fill the resulting vacancy and inhibit the radiative decay process that would give rise to fluorescence emission.
Trappable sensors	Probes that are initially cell membrane permeable but cannot recross the cell membrane after the initial uptake. A common strategy for modifying probes to be trapped in cells involves the incorporation of ester groups to the probe structure. Hydrolysis of the ester moieties by intracellular esterases releases a negatively charged membrane-impermeable form of the probe. Sensor trappability is often critical in tissue imaging experiments, which typically require continuous media perfusion of the biological specimen.

ACRONYMS LIST

NOS	nitric oxide synthase
RNOS	reactive NO species
DPA	di(2-picolyl)amine
DAF	diaminofluorescein
MT	metallothionein
TPEN	*N,N,N′,N′*-tetrakis(2-pyridylmethyl)ethylenediamine
PAECs	pulmonary artery epithelial cells

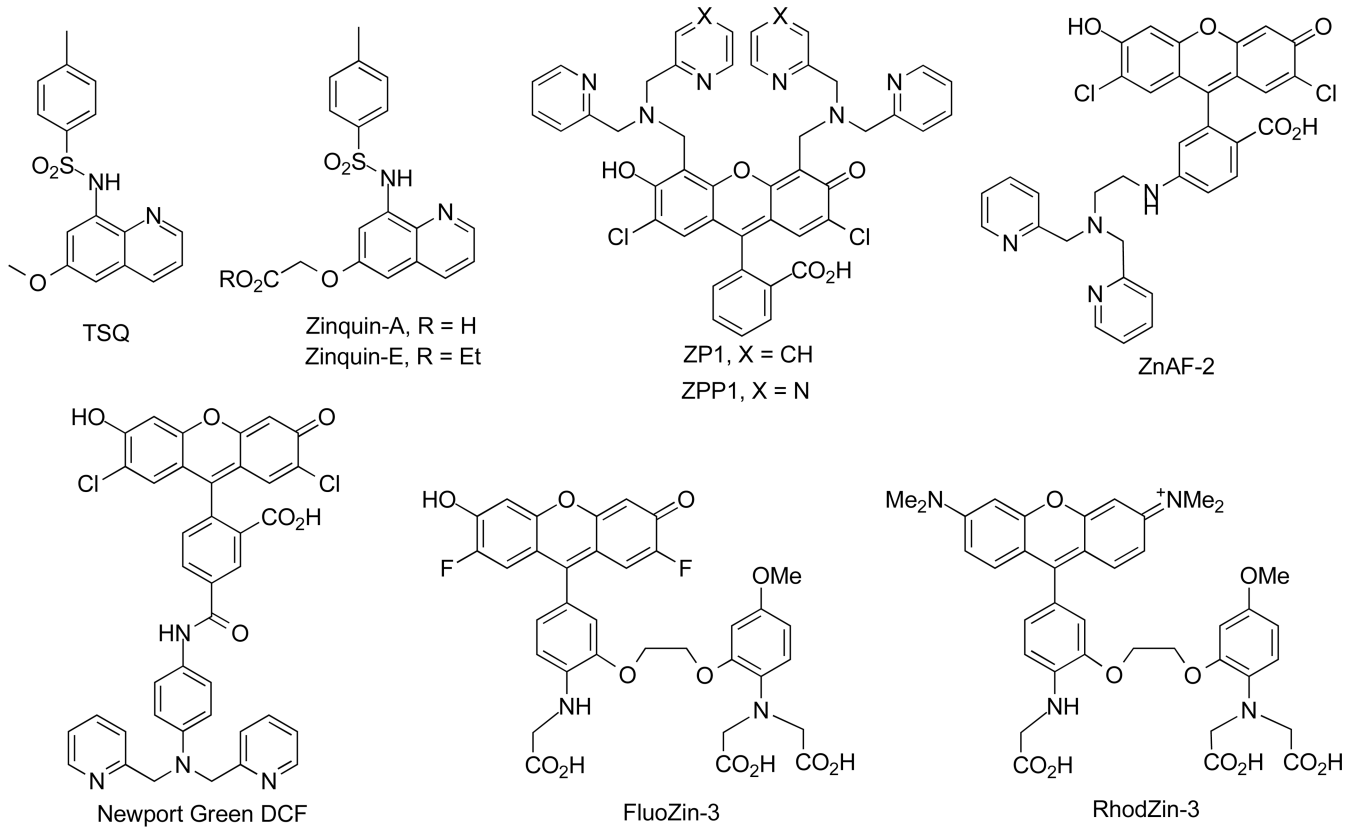

Figure 1.

Selection of fluorescent turn-on sensors for biological zinc. FluoZin-3, RhodZin-3, TSQ, 6-methoxy-8-*p*-toluenesulfonamidequinoline; Zinquin-A, carboxylic acid form of Zinquin; Zinquin-E, ethyl ester form of Zinquin; ZP1, ZPP1, ZnAF-2, Newport Green DCF.

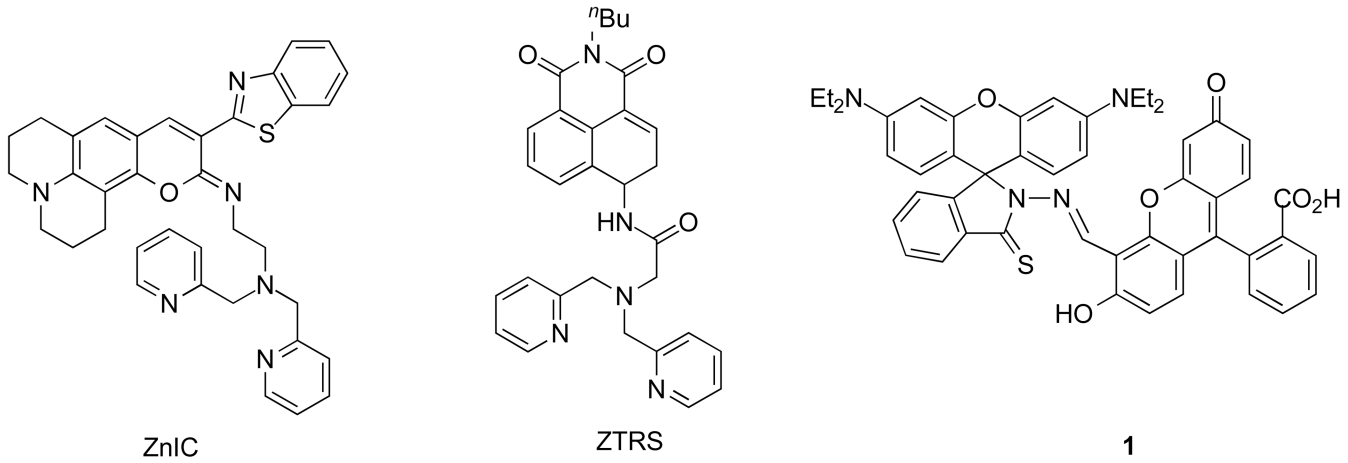

Figure 2.
Selected ratiometric fluorescent probes for biological zinc. Et_2N, *^{n}Bu*, NEt_2, ZnIC, ZTRS, 1, fluorescein-rhodamine construct 1.

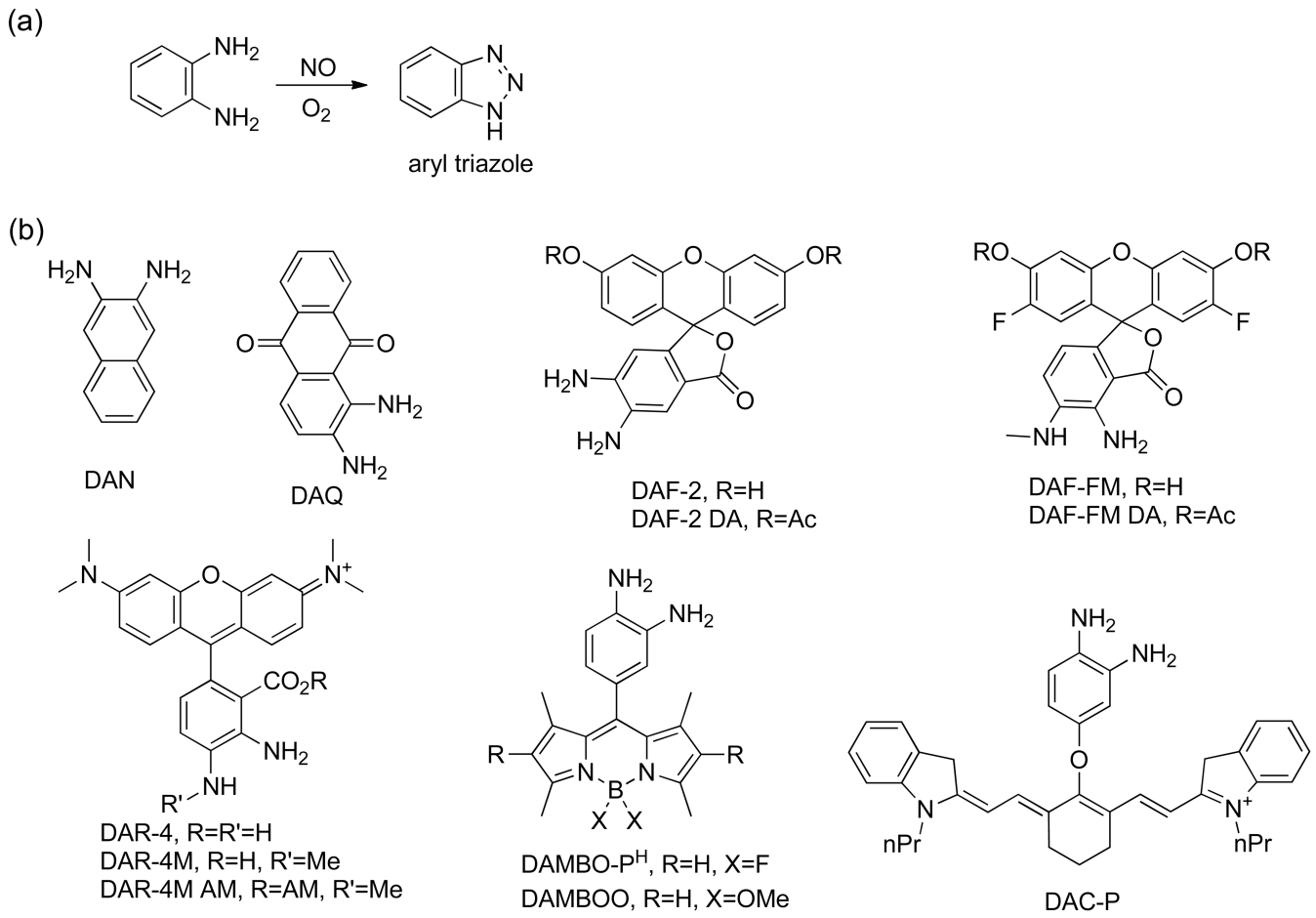

Figure 3.

(*a*) Treatment of *o*-phenylenediamine with NO under aerobic conditions results in triazole formation. (*b*) Fluorescent probes for NO based on *o*-phenylenediamine functionality. DAC-P, DAN, 2,3-diaminonaphthalene; DAF-2, DAF-2 DA, DAF-FM, DAF-FM DA, DAQ, 1,2-diaminoanthraquinone; DAR-4, DAR-4M, DAR-4M AM, DAMBO-P^{H}, DAMBOO, nPr.

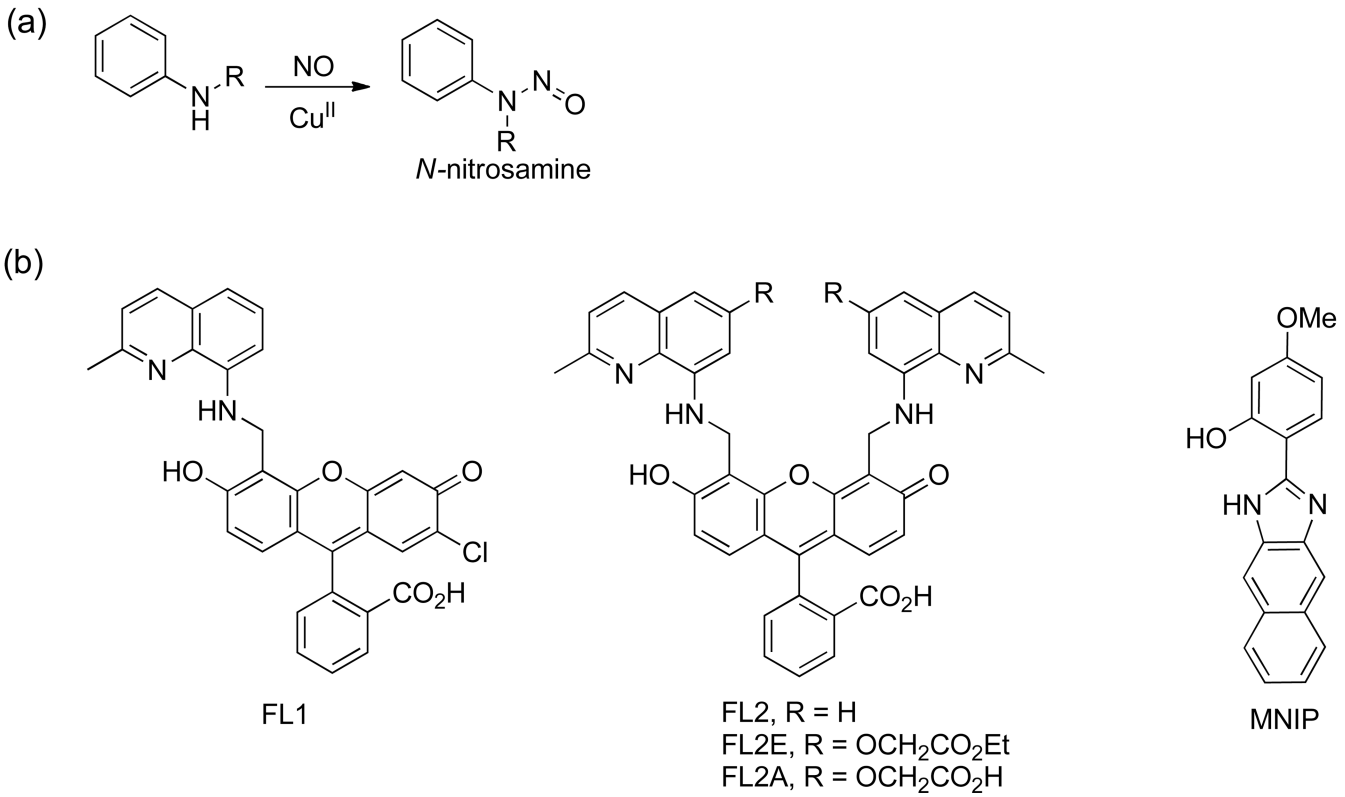

Figure 4.
(*a*) Ligands with secondary amines able to bind Cu(II) are nitrosated upon treatment of NO. (*b*) Fluorescent probes for NO based on Cu(II)-mediated amine nitrosation. FL1, FL2, FL2E, FL2A, MNIP.